X-ray and NMR Conformational Study of Aureobasidin E: A Cyclic Depsipeptide with Potent Antifungal Activity

Akihiko Fujikawa, Yasuko In, Masatoshi Inoue, and Toshimasa Ishida*

Department of Physical Chemistry, Osaka University of Pharmaceutical Sciences, 2-10-65 Kawai, Matsubara, Osaka 580, Japan

Nobuaki Nemoto and Yuji Kobayashi*

Institute for Protein Research, Osaka University, 3-2 Yamadaoka, Suita, Osaka 565, Japan

Ryoichi Kataoka

Computational Science Department, Ryoka System Inc., 1-5-2 Irifune, Urayasu, Chiba 279, Japan

Katsushige Ikai, Kazutoh Takesako, and Ikunoshin Kato

Biotechnology Research Laboratories, Takara Shuzo Co., Ltd., 3-4-1 Seta, Otsu, Shiga 520-21, Japan

Received July 26, 1993 (Revised Manuscript Received November 29, 1993•)

The solid-state and solution conformations of aureobasidin E, a new type of cyclic depsipeptide antibiotic, have been analyzed by X-ray diffraction and NMR spectroscopy to elucidate the possible relationship between its molecular conformation and antifungal bioactivity. The X-ray analysis of the crystal structure recrystallized from hexane–propan-2-ol–acetonitrile [monoclinic, space group $P2_1$, a = 16.458(3) Å, b = 10.638(3) Å, c = 18.133(6) Å, β = 103.51(2)°, Z = 2] shows an arrowhead-like conformation of aureobasidin E stabilized by three transannular N–H···O=C hydrogen bonds, with the formation of three secondary structures of an antiparallel β-sheet, and β- and γ-turns. The conformational analysis by means of NMR spectroscopy performed in DMSO solution and of simulated annealing calculations indicates that the solution structures are, on the whole, homologous to that observed in the solid state in such a way that the molecule forms an arrowhead-like conformation and the βHOMeVal residue, which is indispensable for its bioactivity, is located at the same relative position. However, the ω torsion angle around the βHOMePhe–Pro peptide bond (*cis* orientation in solution and *trans* orientation in solid state) and consequent intramolecular NH···O=C hydrogen bonding formation are different. This leads to the more flexible and rounded conformation of aureobasidin E in solution than in the solid state. The biological roles of some characteristic functional groups in the chemical structure of aureobasidin E are discussed on the basis of molecular conformation.

Introduction

Aureobasidins are complexes isolated from the fermentation broth of *Aureobasidium pullulans* R106.[1] Eighteen structurally related antibiotics, labeled aureobasidin A to R, have so far been isolated from the strain and characterized by the chemical and spectroscopic methods.[2] Aureobasidins, which consist of eight α-amino acid units and one hydroxy acid unit, are classified as a new class of antifungal antibiotics based on the fact that they do not contain fatty acids, compared with the related cyclic depsipeptides so far isolated,[3] all of which contain fatty acids necessary for antifungal activity. In particular, aureobasidins A and E exhibit potent and broad-spectrum antifungal activity, and their potential for clinical use is being vigorously examined because of their low toxicity.

The structural and conformational determination of a bioactive antibiotic is an important first step in addressing the question as to how its biological action is exerted. When information on the interaction with a receptor at the molecular level is lacking, the molecular conformation of the antibiotic itself can provide us with a hypothesis concerning the structure–activity relationship. This would be very helpful in the rational design of a potent new drug.

Keeping these points in mind, this paper reports the solid-state and solution conformations of aureobasidin E (Ab-E) studied by X-ray diffraction and NMR spectroscopy; the preliminary X-ray result has already been reported.[4] Ab-E is a cyclic depsipeptide consisting of 2(*R*)-hydroxy-3(*R*)-methylpentanoic acid (Hmp-1), *N*-methyl-L-valine (MeVal-2 and -7), L-phenylalanine (Phe-3), β-hydroxy-*N*-methyl-L-phenylalanine (βHOMe-Phe-4), L-proline (Pro-5), L-alloisoleucine (aIle-6), L-leucine (Leu-8), and β-hydroxy-*N*-methyl-L-valine (βHOMeVal-9), and

• Abstract published in *Advance ACS Abstracts*, January 1, 1994.

(1) Takesako, K.; Ikai, K.; Haruna, F.; Endo, M.; Shimanaka, K.; Sono, E.; Nakamura, T.; Kato, I. *J.Antibiot.* **1991**, *44*, 919.

(2) (a) Ikai, K.; Takesako, K.; Shiomi, K.; Moriguchi, M.; Umeda, Y.; Yamamoto, J.; Kato, I. *J.Antibiot.* **1991**, *44*, 925. (b) Ikai, K.; Shiomi, K.; Takesako, K.; Mizutani, S.; Yamamoto, J.; Ogawa, Y.; Ueno, M.; Kato, I. *J.Antibiot.* **1991**, *44*, 1187.

(3) (a) Crews, P.; Manes ,L. V.; Boehler, M. *Tetrahedron Lett.* **1986**, *27*, 2797. (b) Chan, W. R.; Tinto, W. F.; Manchand, P. S.; Todaro, L. J. *J.Org.Chem.* **1987**, *52*, 3091. (c) Rowin, G. L.; Miller, J. E.; Albers-Schonberg, G.; Onishi, J. C.; Davis, D.; Dulaney, E. L. *J.Antibiot.* **1986**, *39*, 1772. (d) Mizuno, K.; Yagi, A.; Satoi, S.; Takeda, M.; Hayashi, M.; Asano, K.; Matsuda, T. *J.Antibiot.* **1977**, *30*, 297. (e) Keller-Juslen, C.; Kuhn, M.; Loosli, H. R.; Petcher, T. J.; Weber, H. P.; von Wartburg, A. *Tetrahedron Lett.* **1976**, *17*, 4147. (f) Roy, K.; Mukhopadhyay, T.; Reddy, G. C. S.; Desikan, K. R.; Ganguli, B. N. *J.Antibiot.* **1987**, *40*, 275. (g) Schwartz, R. E.; Giacobbe, R. A.; Bland, J. A.; Monaghan, R. L. *J.Antibiot.* **1989**, *42*, 163. (h) Nishii, M.; Kihara, T.; Isono, K.; Higashijima, T.; Miyazawa, T.; Sethi, S.; McCloskey, J. A. *Tetrahedron Lett.* **1980**, *21*, 4627.

(4) Ishida, T.; In, Y.; Fujikawa, A.; Urata, H.; Inoue, M.; Ikai, K.; Takesako, K.; Kato, I. *J. Chem. Soc. Chem. Commun.* **1992**, 1231.

0022-3263/94/1959-0570$04.50/0

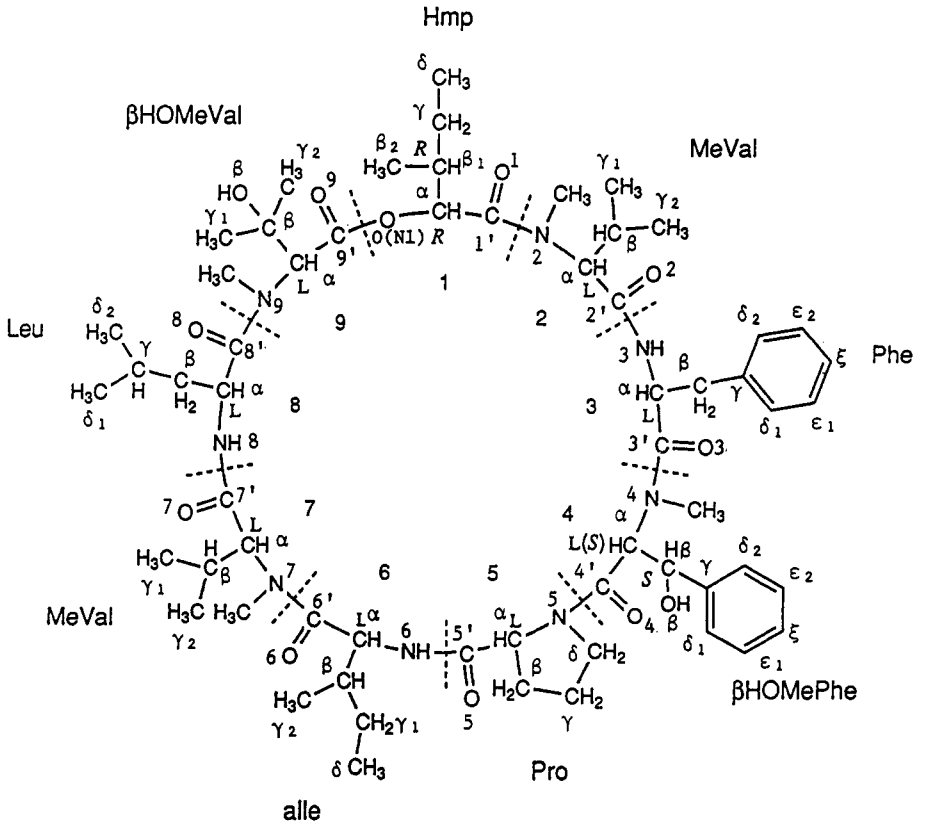

Figure 1. Chemical structure of Ab-E, together with atomic numbering used in this study.

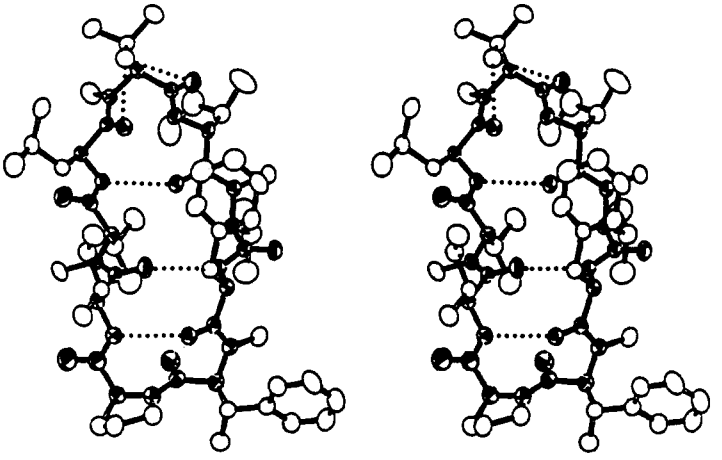

Figure 2. A stereoscopic view of Ab-E molecular conformation. The backbone chain is represented by the detailed thermal ellipsoids and thick bonds. Intramolecular hydrogen bonds are shown by dotted lines.

is different from Ab-A only at position 4 (MePhe-4 for Ab-A). The chemical structure and atomic numbering of Ab-E are shown in Figure 1. Judging from the antifungal activities of Ab-A to -R,[1] it could be said that the N-methylation of amide bonds (four out of seven) and the OH group of βHOMeVal-9 are indispensable for its biological activity.

Results

Solid-State Structure and Conformation. A stereoscopic ORTEP[5ab] view of Ab-E is shown in Figure 2, where the side chains of respective residues are depicted with open ellipsoids and the intramolecular NH···O=C hydrogen bonds are shown by dotted lines. The conformational torsion angles of backbone and side chains are listed in Table 1, in which the averaged torsion angles of the seven well-conserved structures in solution derived from NMR spectroscopy and simulated annealing (SA) calculations (discussed later) are also listed for comparison. The hydrogen bonding parameters are given in Table 2.

Because of the relatively high thermal motions of the side-chain terminal atoms of each residue, the estimated standard deviation (ESD) values for bond lengths (0.005–0.1 Å) and bond angles (0.2–0.5°) are somewhat larger than usual. However, these geometric parameters are

(5) (a)Johnson, C. K. ORTEP II: Report ORN-5138; Oak Ridge National Laboratory: Tennessee, 1976. (b) The author has deposited atomic coordinates for this structure with the Cambridge Crystallographic Data Centre. The coordinates can be obtained, on request, from the Director, Cambridge Crystallographic Data Centre, 12 Union Road, Cambridge, CB2 1EZ, UK.

Table 1. Conformational Torsion Angles (deg) of Ab-E in Solid State[a] and DMSO Solution[b]

residue		X-ray crystal	NMR solution
Hmp-1	ϕ[c]	137.4(4)	81(3)
	ψ	-174.1(4)	-157(1)
	ω	-168.1(4)	-173(2)
	$\chi^{1,1}$	-26.1(5)	-49(5)
	$\chi^{1,2}$	93.4(5)	75(5)
	$\chi^{2,1}$	-59.8(6)	-167(2)
MaVal-2	ϕ	-113.6(4)	-133(6)
	ψ	109.9(4)	91(4)
	ω	-171.9(4)	169(1)
	$\chi^{1,1}$	-53.1(5)	-56(10)
	$\chi^{1,2}$	-174.9(5)	-172(2)
Phe-3	ϕ	-129.9(4)	-82(4)
	ψ	70.4(4)	-84(2)
	ω	-175.1(5)	179(1)
	χ^{1}	-51.4(4)	-179(1)
	$\chi^{2,1}$	99.4(5)	64(2)
	$\chi^{2,2}$	-79.3(6)	-114(2)
βHOMePhe-4	ϕ	50.0(4)	-163(1)
	ψ	-122.8(5)	109(1)
	ω	-170.2(5)	-14(1)
	$\chi^{1,1}$	-44.6(4)	-68(1)
	$\chi^{1,2}$ [d]	-164.0(4)	58(1)
	$\chi^{2,1}$	94.3(5)	100(1)
	$\chi^{2,2}$	-86.1(5)	-79(1)
Pro-5	ϕ	-82.3(5)	-104(1)
	ψ	5.0(5)	47(1)
	ω	174.7(5)	-168(1)
	χ^{1} [e]	35.7(5)	34(1)
	χ^{2} [f]	-37.6(5)	-37(1)
	χ^{3} [g]	24.6(5)	25(1)
	χ^{4} [h]	-2.2(4)	-4(1)
	χ^{5} [i]	-21.1(4)	-18(1)
aIle-6	ϕ	-106.2(5)	-85(2)
	ψ	112.8(4)	124(3)
	ω	175.6(5)	-179(2)
	$\chi^{1,1}$	175.0(4)	177(1)
	$\chi^{1,2}$	-63.1(4)	-61(1)
	χ^{2}	-173.2(5)	-167(1)
MeVal-7	ϕ	-116.5(4)	-103(2)
	ψ	91.1(4)	75(5)
	ω	-163.6(5)	-176(6)
	$\chi^{1,1}$	-49.1(5)	-51(2)
	$\chi^{1,2}$	-171.8(5)	-173(3)
Leu-8	ϕ	-148.5(4)	-153(7)
	ψ	99.5(4)	118(8)
	ω	-173.1(4)	-169(1)
	χ^{1}	-164.4(5)	-171(5)
	$\chi^{2,1}$	173.5(5)	74(10)
	$\chi^{2,2}$	-62.3(5)	-162(10)
βHOMeVal-9	ϕ	49.0(4)	58(7)
	ψ[j]	41.9(3)	48(5)
	ω[k]	161.1(4)	175(5)
	$\chi^{1,1}$	-50.2(4)	-49(6)
	$\chi^{1,2}$	-169.4(4)	-166(4)
	$\chi^{1,3}$ [l]	70.1(4)	74(4)

[a] The ESD values of X-ray torsion angles are given in parentheses. [b] Values correspond to the average of seven well-converged solution structures. [c] C(9')-O(N1)-C(1α)-C(1'). [d] N(4)-C(4α)-C(4β)-O(4β). [e] N(5)-C(5α)-C(5β)-C(5γ). [f] C(5α)-C(5β)-C(5γ)-C(5δ). [g] C(5β)-C(5γ)-C(5δ)-N(5). [h] C(5γ)-C(5δ)-N(5)-C(5α). [i] C(5δ)-N(5)-C(5α)-C(5β). [j] N(9)-C(9α)-C(9')-O(N1). [k] C(9α)-C(9')-O(N1)-C(1α). [l] N(9)-C(9α)-C(9β)-O(9β).

unexceptional and compare well with those of other similar-size molecules such as didemnin B[6] and swinholide A.[7] No abnormality caused by the ring formation was observed for the Cα bonding parameters of respective residues.

No notable characteristics were observed for the conformational torsion angles of Ab-E. The peptide groups

Table 2. Hydrogen Bonds and Short Contacts with ESD in Parentheses

donor at x,y,z (D-H)	acceptor (A)	length (Å) (D···A)	symmetry operation of A
	Possible Hydrogen Bonds		
N(3)	O(6)	2.887(5)	x,y,z
N(6)	O(3)	3.099(5)	x,y,z
N(8)	O(1)	2.966(5)	x,y,z
O(9β)	O(8)	2.735(5)	x,y,z
O(9β)	O(9)	3.088(5)	x,y,z
O(4β)	O(4)	2.688(6)	$1-x,y+1/2,-z$
	Short Contacts		
O(N1)	O(8)	2.976(5)	x,y,z
O(4β)	N(5)	3.174(6)	x,y,z
N(5)	O(3)	3.041(5)	x,y,z
N(6)	O(4)	3.156(6)	x,y,z
O(N1)	O(1)	2.611(5)	x,y,z
N(4)	O(4)	2.836(6)	x,y,z
N(9)	O(N1)	2.665(5)	x,y,z

are all *trans* and are nearly planar with the maximum $\Delta\omega$ of 16.4° at MeVal-7. The ester linkage between the βHOMeVal-9 and Hmp-1 residues also assumes a *trans* orientation (=161.1°). The ϕ_i/ψ_i torsion angles for each residue, except for the Hmp-1, are all in the well-defined low-energy region on a Ramachandran map. The ϕ angle of Hmp-1 is rarely observed for the usual amino acid residue, and this could be explained as the effect of an ester linkage, instead of an amide one.

The backbone conformation of Ab-E can be divided into three types of secondary structures, *i.e.*, an antiparallel β-sheet structure, and β- and γ-turn structures. The Hmp–MeVal–Phe and aIle–MeVal–Leu sequences form an antiparallel β-sheet structure stabilized by three hydrogen bonds of [Phe]NH···O=C[aIle], [aIle]NH···O=C[Phe], and [Leu]NH···O=C[Hmp], although the ϕ/ψ torsion angles of these sequences somewhat deviate from the standard values of $\phi = \sim -139°$ and $\psi = \sim 135°$.[8] On the other hand, the Phe–βHOMePhe–Pro–aIle sequence forms a typical Type II' β-turn structure, in which the βHOMePhe–Pro sequence is located at the corner of the bend. This structure is stabilized by an intramolecular hydrogen bond of [aIle]NH···O=C[Phe] and by two electrostatic short contacts of [Pro]N···O=C[Phe] and [aIle]NH···O=C[βHOMePhe] (Table 2). The Leu–βHOMeVal–Hmp sequence forms a kind of γ-turn structure with the βHOMeVal residue at the corner, although the ϕ/ψ torsion angle significantly deviates from the usual turn (ϕ = 70–80°, ψ = –60–70°) or inverse turn (ϕ = –70—85°, ψ = 60–70°)[9] because of the lack of any intramolecular hydrogen bond due to the N-methylation of βHOMeVal residue; this ϕ/ψ torsion angle, rather, is observed in the left-handed α-helix conformation ($\phi = \sim 57°$, $\psi = \sim 47°$) found frequently in peptides containing the uncommon amino acid Aib (α-aminoisobutyric acid).[10] The OH group of βHOMeVal-9 is hydrogen-bonded to two O=C groups of Leu-8 and βHOMeVal-9 in a bifurcated manner. These hydrogen bonds, together with the [Hmp]O(N1)···N(9)-[βHOMeVal] electrostatic short contact, stabilize the γ-turn structure.

By virtue of these three secondary structure elements, Ab-E forms an arrowhead-like conformation, wherein the βHOMeVal-9 residue is located at the corner. The side-chain conformations of each residue, except for Hmp-1, are all in the range of the allowed (χ^1, χ^2) distribution,

(6) Hossain, M. B.; van der Helm, D.; Antel, J.; Sheldrick, G. M.; Sanduja, S. K.; Weinheimer, A. J. *Proc. Natl. Acad. Sci. U.S.A.* **1988**, *85*, 4118.
(7) Doi, M.; Ishida, T.; Kobayashi, M.; Kitagawa, I. *J. Org. Chem.* **1991**, *56*, 3629.
(8) Arnott, S.; Dover, S. D.; Elliot, A. *J. Mol. Biol.* **1967**, *30*, 201.
(9) Nemethy, G.; Printz, M. P. *Macromolecules* **1972**, *5*, 755.
(10) Arnott, S.; Dover, S. D. *J.Mol.Biol.* **1967**, *30*, 209.

although those of aIle-6 and Leu-8 belong to the lowest population region surveyed for peptides and proteins.[11] The $\chi^{1,1}$ and $\chi^{1,2}$ torsion angles of Hmp-1 somewhat deviate from the usual Ile side-chain conformation ($\chi^{1,1} = \sim -60°$, $\chi^{1,2} = \sim 60°$), probably due to the ester linkage of Hmp residue. The pyrrolidine ring of Pro-5 has the usual Cβ-*exo*-Cγ-*endo* puckering (C_2-conformation).[12]

In the crystal structure of Ab-E molecules, no solvents of crystallization are contained. The crystal structure forms a hollow due to stacking of Ab-E ring structures. Only hydrogen bonds are intermolecularly formed between the OH and O=C groups of the βHOMePhe residues related by the diad-screw symmetry. Thus, the crystal structure is mainly stabilized by the van der Waals forces among the neighboring molecules. This is the reason why Ab-E has relatively high temperature coefficients for the side-chain atoms.

Conformational Analysis of Ab-E in Solution. ^{1}H NMR Assignment. All proton peak assignments of Ab-E in DMSO-d_6 were performed by the sequence-specific assignment procedure,[13] based on the connectivity information *via* the scalar coupling in the phase-sensitive DQF-COSY (double quantum filtered chemical-shift correlated spectroscopy) experiments and the sequential NOE networks along the peptide backbone protons.

Resonances belonging to the same residues were identified using DQF-COSY and HOHAHA (homonuclear Hartmann–Hahn) spectra. The sequential network of NOEs along the peptide backbone $C_\alpha H$, NH, or NCH_3 protons was traced in the NOESY spectra (Figure 3). The connectivity between the βHOMeVal-9 and Hmp-1 residues was identified by the distinct NOE between the CαH-[βHOMeVal] and CγCH_3 [Hmp] protons. Concerning the connectivity between the βHOMePhe-4 and Pro-5 residues, the distinct NOEs between their CαH protons were observed (Figure 4), clearly indicating the predominant *cis* orientation around the βHOMePhe–Pro amide bond, as was reported by Wüthrich.[13]

As is shown in Figure 5A, Ab-E in DMSO-d_6 showed a mixture of *cis*/*trans* isomers around the βHOMePhe–Pro amide bond. The *cis* conformers exist overwhelmingly in the DMSO solution, and the ratio of *cis*/*trans* isomers is about 4/1, as judged from the intensities of NH protons in each isomer. Thus, only the *cis* isomer was considered in the subsequent conformational analysis of Ab-E. It was difficult to completely assign all proton resonances and measure the NOE intensities to analyze the conformation of *trans* isomer in solution. Table 3 summarizes the proton chemical shifts of respective residues corresponding to the *cis* isomer. When they were compared with the chemical shifts of Ab-E in chloroform,[14] no significant differences were observed.

Vicinal Coupling Constants and Temperature Dependence of NH Protons. To obtain information on the ϕ torsion angles around the N_iH–$C_{i\alpha}H$ bonds, the vicinal proton coupling constants ($^3J_{NHC\alpha H}$) were estimated according to Kim and Prestegard,[15] and possible ϕ angles

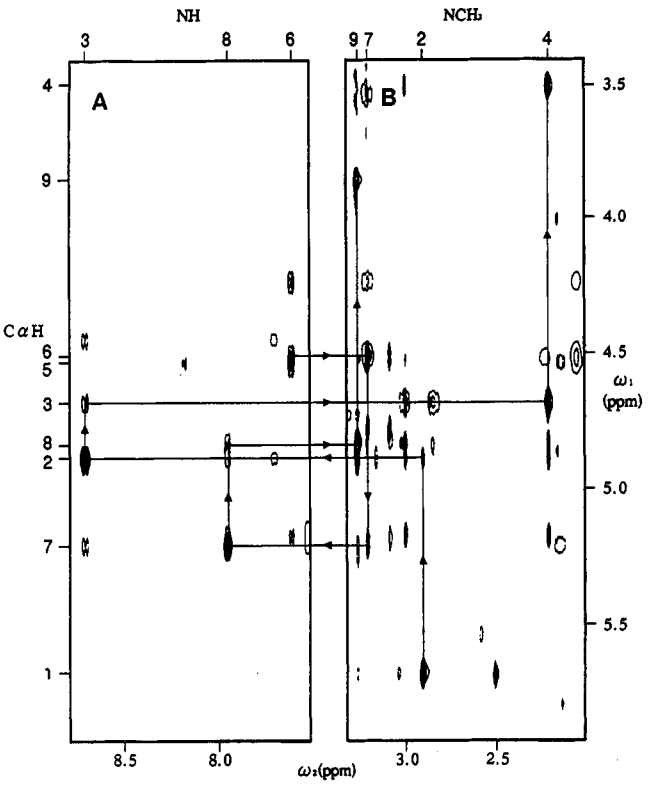

Figure 3. Partial sequential connectivity of Ab-E *via* $d_{C\alpha NH}$ (A) and $d_{C\alpha NCH3}$ (B) by NOESY spectrum with a mixing time of 400 ms. The cyclic assignment pathway is indicated with straight lines and arrows, leading from the circled intraresidual CαH (Hmp-1)–NCH_3(MeVal-2) cross peak clockwise around the structure of Figure 1 and back to the initial point. The chemical shifts of the individual amide protons and *N*-methyl groups are indicated at the top and identified by the sequence positions (Figure 1). On the left, the same information is given for the Cα protons.

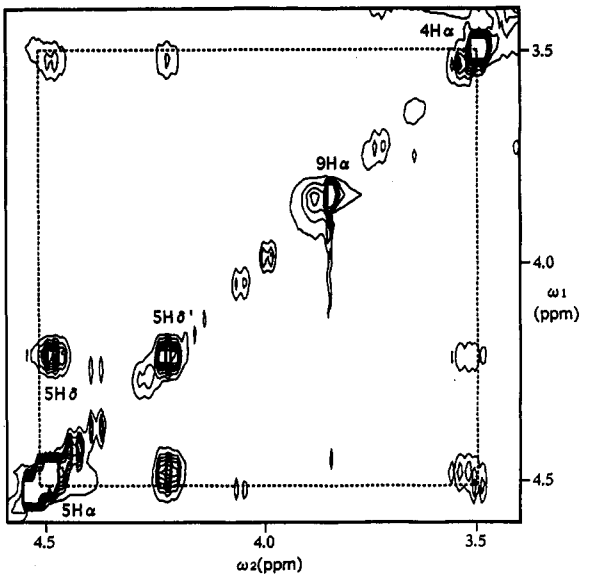

Figure 4. NOE cross peak of Hα(βHOMePhe)–Hα(Pro) observed in the *cis* isomer.

were estimated using a Karplus-type equation.[16] The results are given in Table 4, where the averaged angles of the 40 converged structures derived from the SA calculations (discussed later) are given for comparison. Fur-

(11) (a) Bhat, T. N.; Sasisekharan, V.; Vijayan, M. *Int.J.Pept. Protein Res.* **1979**, 13, 170. (b) Benedetti, E.; Morelli, G.; Némethy, G.; Scheraga, H. A. *Int. J. Pept. Protein Res.* **1983**, *22*, 1.
(12) Ashida, T.; Kakudo, M. *Bull. Chem. Soc. Jpn.* **1974**, *47*, 1129.
(13) Wüthrich, K. *NMR of Proteins and Nucleic Acids*; John Wiley & Sons: New York, 1986.
(14) Ikai, K.; Shiomi, K.; Takesako, K.; Kato, I.; Naganawa, H. *J.Antibiot.* **1991**, *44*, 1199.
(15) Kim, Y.; Prestegard, J. H. *J.Magn.Res.* **1989**, *84*, 9.
(16) Pardi, A.; Billeter, M.; Wüthrich, K. *J.Mol.Biol.* **1984**, *180*, 741.

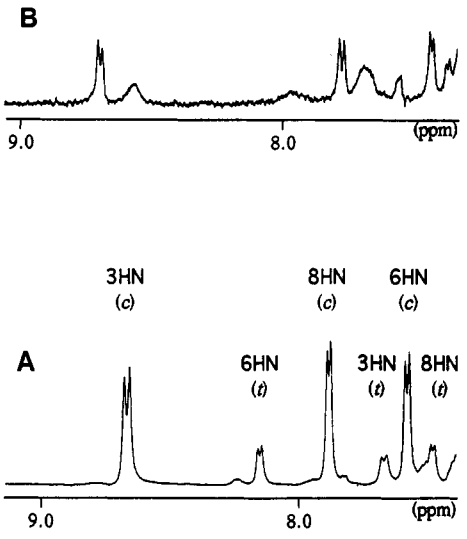

Figure 5. *Cis/trans* population around βHOMePhe–Pro amide bond observed for the Phe-3, aIle-6, and Leu-8 NH proton chemical shifts in DMSO-d_6 (A) and hexane–propan-2-ol–acetonitrile (B) solutions. The italicized letters *c* and *t* represent the *cis* and *trans* isomers, respectively.

Table 3. Resonance Assignments and Chemical Shifts for Ab-E in DMSO-d_6 Solution

	chemical shifts (ppm)			
residue	NH or NCH_3	CαH	CβH	others
Hmp-1	–	5.64	1.79	γCH_2 1.02, 1.35; γCH_3 0.89; δCH_3 0.74
MeVal-2	2.89	4.87	1.88	γCH_3 0.66, 0.73
Phe-3	8.71	4.67	2.82	δCH 7.10; εCH 7.35; ζCH 7.20
βHOMe-Phe-4	2.21	3.49	5.14	δCH 6.93; εCH 7.23; ζCH 7.26; βOH 6.07
Pro-5	–	4.54	1.90	γCH_2 1.90, 2.06; δCH_2 4.22, 4.48
aIle-6	7.59	4.49	2.23	γCH_2 1.09, 1.41; γCH_3 1.13; δCH_3 0.88
MeVal-7	3.20	5.19	2.14	γCH_3 0.71, 0.81
Leu-8	7.94	4.81	1.23 1.55	γCH 1.42; δCH_3 0.86, 0.88
βHOMeVal-9	3.25	3.83	–	γCH_3 1.21, 1.25; βOH 4.71

Table 4. Temperature Coefficients of NH and βOH Protons, and Vicinal Coupling Constants between NH and CαH Protons and Corresponding φ Torsion Angles (deg), Together with Averaged Angles of 40 Structures Converged by SA Calculations

residue	-Δδ/d*T*, ppb/K
Phe-3 NH	4.02
βOHMePhe-4 βOH	4.94
aIle-6 NH	1.59
Leu-8 NH	5.03
βOHMeVal-9 βOH	0.38

residue	$^3J_{NHC\alpha H}$, Hz	ϕ_{exp},* deg	ϕ_{SA}, deg
Phe-3	7.4	−154, −86	−81 ± 10
aIle-6	8.3	−146, −94	−86 ± 7
Leu-8	8.7	−142, −98	−139 ± 13

* The values were calculated from the equation of $^3J_{HN\alpha H} = 1.9–1.4 \cos\theta + 6.4 \cos^2\theta$, where $\phi = |\theta - 60|°$.

thermore, in order to estimate the environment in which the amide and hydroxyl protons are located, the temperature dependences of NH and βOH proton chemical shifts were measured in the range from 20 °C to 60 °C at intervals of 10 °C, and temperature coefficients were obtained from the least-squares plots (Table 4). Generally, NH protons showing -dδ/d*T* values of less than approximately 4 ppb/K are considered to be participating in hydrogen bonding.[17]

Secondary Structure. The NOE connectivities observed in the Ab-E are shown in Figure 6. The proton–proton NOE facilitates not only the sequential peak assignment but also the elucidation of some regular secondary structures. Because of the N-methylation of four out of seven amide bonds, information concerning the secondary structure is severely limited. However, the NOE intensity pattern of $d_{\alpha N(i,i+1)}$ [or $d_{\alpha NQ(i,i+1)}$] and $d_{NN(i,i+1)}$ [or $d_{NNQ(i,i+1)}$] observed in MeVal–Phe–βHOMePhe and aIle–MeVal–Leu–βHOMeVal showed the extended β structures of these sequences.[13] On the other hand, a turn structure around the βHOMePhe–Pro sequence is recognized by the NOE between the Phe-3 and aIle-6 NH protons ($d_{NN(i,i+3)}$). This turn structure is further suggested by the low dδ/d*T* value of aIle-6 NH proton; the NH proton could be hydrogen-bonded to the carboxyl oxygen atom of Phe-3.

Three-Dimensional Structure Calculation. In order to elucidate the three-dimensional structure of Ab-E, the simulated annealing (SA) calculation[18] was performed by adjusting the force constant. Starting with 50 different sets of conformations with random arrays of atoms, to eliminate any possible source of initial bias in the folding pathway, the energy-minimization trials gave 50 satisfactory conformers. The convergence analysis of these 50 structures is given in Figure 7, *i.e.*, the statistical distributions as a function of RMS (root-mean-square) violation, the ω distributions of respective residues, and the (φ,ψ) plots of the backbone conformations. Among them, 40 structures, which were converged to less than 0.8 and 0.12 Å for the averaged RMS distance deviation of backbone chains and the averaged RMS violation of overall structures, respectively, were selected for consideration of the conformation of Ab-E in solution. The superposition of their structures is shown in Figure 8 and their structural statistics are given in Table 5. As could be supposed from Figure 8 and the (φ,ψ) plots of respective residues (supplementary material), the conformation of Hmp–MeVal–Phe–βHOMePhe backbone chain shows a relatively high flexibility compared with that of the remaining chain, and several kinds of orientations could be formed. Consequently, the solution structure takes more flexible and rounded conformations than the slim and tight X-ray crystal structure. Two conformers, which represent the large conformational variation among 40 conformers, are shown in Figure 9, where the intramolecular hydrogen bonds are shown by dotted lines.

Comparison with X-ray Structure. In order to compare the conformation of Ab-E in solution with its X-ray crystal structure, 7 conformers, which show the best pairwise RMS deviations of <0.2 Å for Cα atoms among 40 solution structures, were chosen. Figure 10 shows the superimposition of these structures (shaded lines) on the X-ray structure (solid line) with respect to the best fit of the backbone atoms of all residues. The averaged conformational torsion angles of the former structures are given in Table 1.

(17) (a) Ohnishi, M.; Urry, D. W. *Biochem. Biophys. Res. Commun.* **1969**, *36*, 194. (b) Urry, D. W.; Long, M. M. *CRC Crit. Rev. Biochem.* **1976**, *6*, 1.

(18) (a) Clore, G. M.; Nigles, M.; Sukumaran, D. K.; Brunger, A. T.; Karplus, M.; Gronenborn, A. M. *EMBO J.* **1986**, *5*, 2729. (b) Nilges, M.; Clore, G.M.; Gronenborn, A. M. *FEBS Lett.* **1988**, *229*, 317.

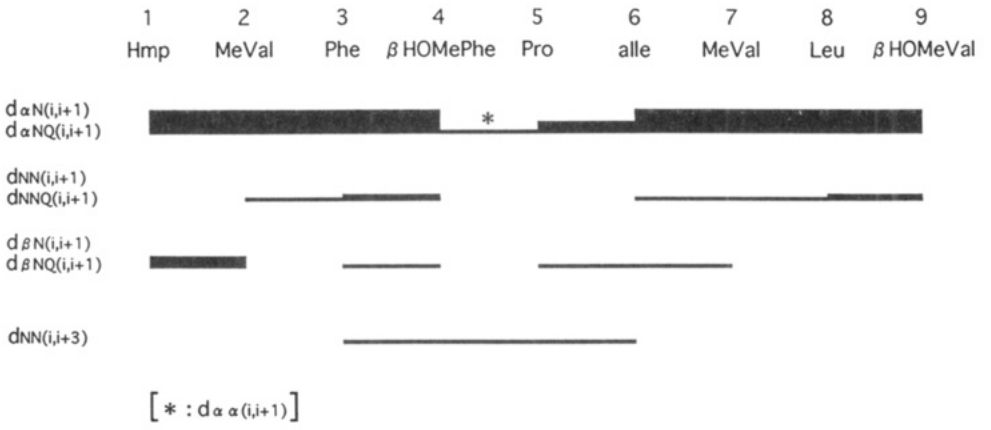

Figure 6. Inter-residual NOE intensities in the NOESY data with a mixing time of 400 ms measured in DMSO-d_6 solution. The degree of intensity is represented by the thickness of the line. Symbols α, β, N, and NQ represent CαH, CβH, NH, and NCH_3 protons, respectively.

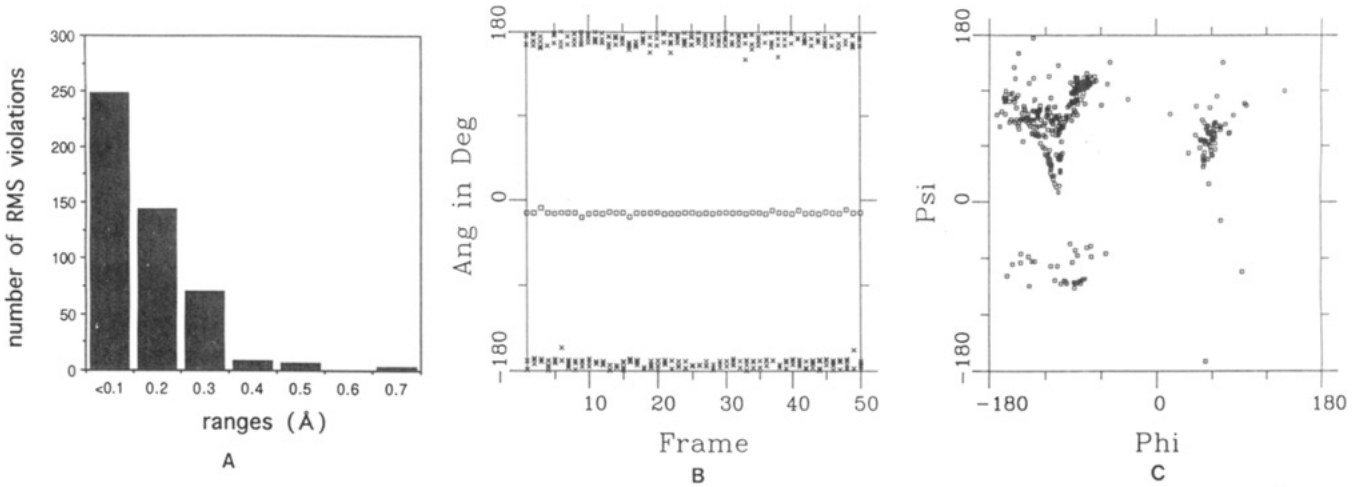

Figure 7. Convergence analysis of Ab-E solution structures by the statistical distribution as a function of RMS violation (A), the ω distribution (B), and (ϕ,ψ) plots (C) of 50 calculated structures. The squares in B represent the torsion angles of βHOMePhe–Pro amide bond.

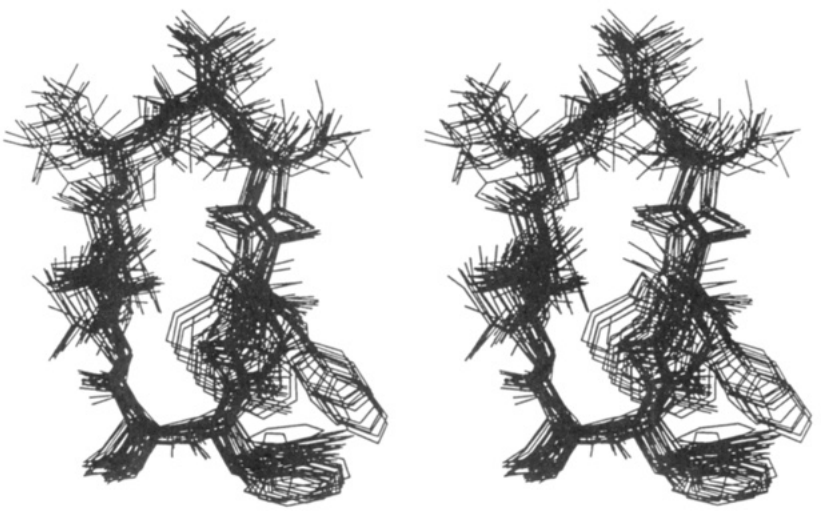

Figure 8. Stereoscopic best-fit superposition of the 40 converged structures.

Discussion

The conformational analysis of Ab-E, a new type of potent antifungal antibiotic, is of special importance for elucidating the structure–activity relationship and for effectively developing clinically useful drugs. The crystal structure of Ab-E showed a unique arrowhead-like conformation, which is composed of three secondary structures of an antiparallel β-sheet, and β- and γ-turns, and is stabilized by three transannular NH···O=C hydrogen bonds. This characteristic conformation gives us a clue to the reason why four out of the seven amide bonds have to be methylated to manifest the biological activity. These N-methylations may be necessary to form only one well-

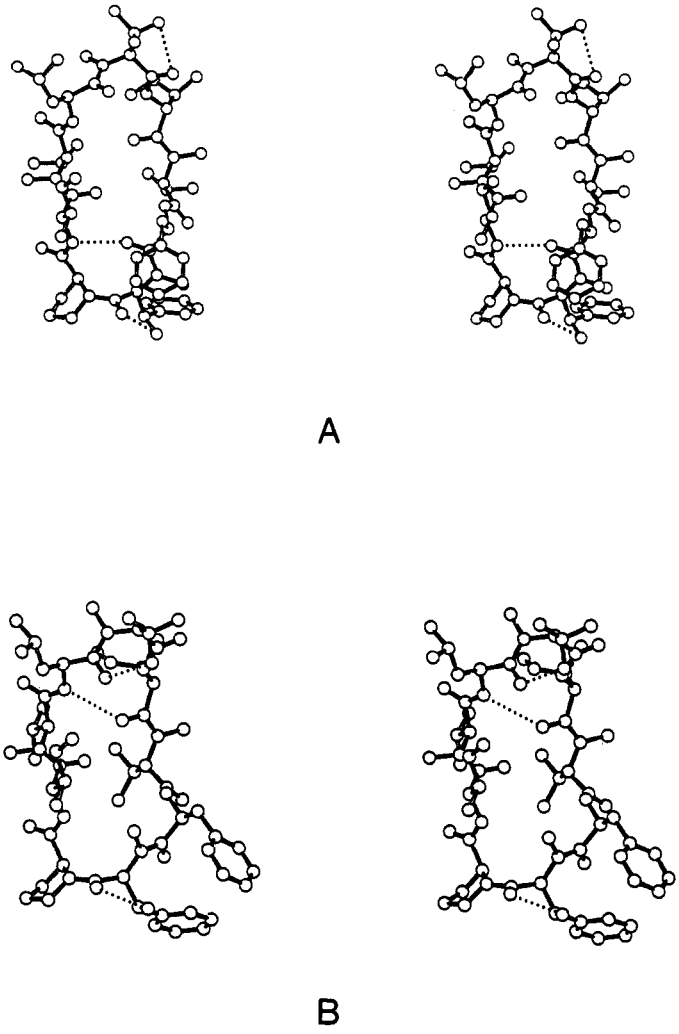

Figure 9. Stereoscopic views of two representative conformers in solution showing the large conformational variations between each other among the 40 converged structures. The dotted lines represent hydrogen bonds.

Table 5. Averaged RMS Violation, RMS Deviation, and Calculated Energy Values of 40 Converged Structures, Together with Comparison with X-ray Structure

	average value ± standard deviation
RMS violation	0.117 ± 0.008 Å
RMS deviation (backbone)	0.764 ± 0.264 Å
energies	
forcing potential	4.65 ± 0.40 kcal/mol
bond	49.95 ± 0.97 kcal/mol
van der Walls	133.14 ± 2.69 kcal/mol
distance difference from X-ray structure	
all atoms	2.86 ± 0.22 Å
heavy atoms	2.39 ± 0.19 Å
backbone	0.86 ± 0.15 Å
Cα	0.87 ± 0.17 Å
energy difference from X-ray structure	
total	12.57 kcal/mol
bond	0.59 kcal/mol
van der Waals	2.68 kcal/mol
Coulombic	2.56 kcal/mol
NOE + dihedral	−1.11 kcal/mol

defined conformation such as that shown in Figure 2. Otherwise, some other conformations with different combinations of intramolecular NH···O=C hydrogen bonds would be possible.

The crystal conformation also showed a characteristic feature for the βHOMeVal-9 conformation, *i.e.*, this residue is located at the tip of an arrowhead-like structure and the βHO group is tightly fixed with the bifurcated hydrogen bonds. Since it is known that lack of this OH group leads to a significant decrease in biological activity,[1] this conformational situation of the βHOMeVal-9 residue may be necessary for manifestation of its activity or for binding to the receptor.

The conformational analysis of Ab-E in solution showed that, in spite of the limited data and resolution for the structure analysis, the Ab-E molecule assumes some conserved conformations in DMSO solution. As judged from the well-converged seven structures displayed in Figure 10, it could be said that conformations of Ab-E molecule in solution, as a whole, are essentially the same as that observed from the X-ray crystal structure (Table 1), although they are much more flexible and rounded (Figures 8 and 9). The ϕ torsion angles estimated from the $^3J_{NHC\alpha H}$ coupling constants coincide well with those of the SA converged structures (Table 4). Also, most of these structures appear to account for the temperature coefficients of NH protons (Table IV), *i.e.*, the aIle-6 NH proton showing the lowest $d\delta/dT$ values is assigned to the intramolecular hydrogen bond of [aIle]NH···O=C[Phe] involved in the β-turn structure; about two-thirds of 40 solution conformers assume the β-turn structures of [aIle]-NH···O=C[Phe] such as that in Figure 9(A).

One of the most significant differences between the solid-state and solution conformations is the *cis/trans* orientation around the βHOMePhe–Pro bond. As is shown in Figure 5, parts A and B, Ab-E exists as an equilibrium mixture of *cis* and *trans* isomers, and its *cis/trans* ratio is solvent-dependent: about 4/1 in DMSO solution and about 1/2 in the crystallization mixture (hexane/propan-2-ol/acetonitrile).[19] This reflects the fact that the *cis/trans* conformational transition around the βHOMePhe–Pro bond is reversible in spite of the constraint imposed on the ring structure of the Ab-E molecule. The βOH group of the βHOMePhe-4 residue appears to play an important role in stabilizing both *cis* and *trans* conformations of Ab-E. In the crystal structure, this OH group forms an intermolecular hydrogen bond with the neighboring carbonyl oxygen atoms. The fixation of the βHOMePhe side chain by this hydrogen bond could be necessary for the *trans* conformation to avoid the steric hindrance occurring between this side chain and the Pro-5 pyrrolidine ring. On the other hand, all structures of Ab-E in DMSO solution form an intramolecular hydrogen bond between the β-OH and O=C groups of βHOMePhe-4, thus stabilizing the *cis* conformation (Figure 9).

Most of the 40 converged structures, unlike the X-ray structure, show no simultaneous hydrogen bond formations of [Leu]NH···O=C[Hmp] and [Phe]NH···O=C[aIle], and consequently the β-sheet structure formed between the Hmp–MeVal–Phe and aIle–MeVal–Leu sequences is not as straight as that of the X-ray structure, but is rather rounded. This leads to a conformational equilibrium between the structures shown in Figure 9 parts A and B. The $d\delta/dT$ values of Phe and Leu residues appear to reflect this situation, where their amide protons are located at the interior of the ring structure. On the other hand, the much lower $d\delta/dT$ value of the βHO proton in βHOMeVal-9

(19) Respective peaks corresponding to *cis* and *trans* isomers in the crystallization solvent were not experimentally assigned. However, it could be assumed that only the *trans* isomer was crystallized from the mixture of *cis* and *trans* isomers under the present recrystallization conditions.

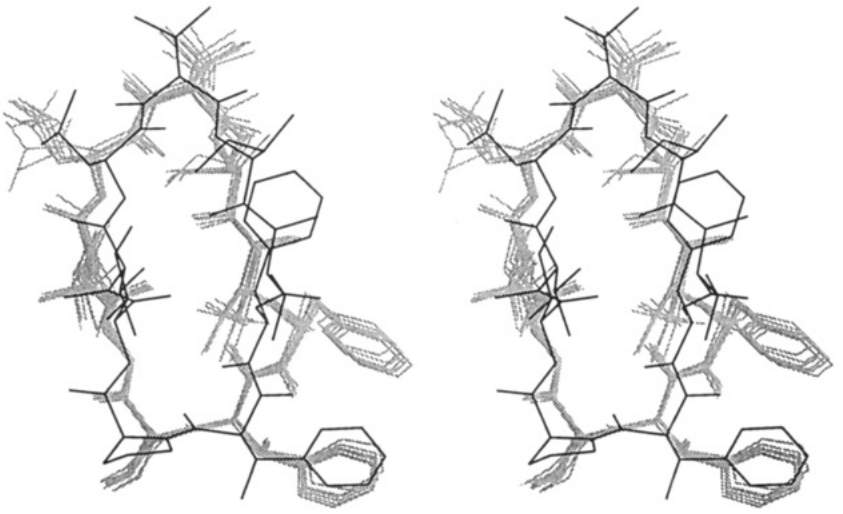

Figure 10. Stereoscopic view of conformational comparison of the seven converged solution structures (shaded lines) with the X-ray crystal structure (solid lines).

than that in βHOMePhe-4 arises from hydrogen bond formation, indicating the conformational rigidity around the βHOMeVal-9 residue.

Apart from the above-mentioned conformational differences, the Ab-E molecule shows the following similar characteristics in the conformations in solid and solution states (Figure 10). The elemental secondary structures of an antiparallel β-sheet, and β- and γ-turns, are formed similarly in both states. Consequently, the arrowhead-like structure, at the tip of which the βHOMeVal residue is located, is commonly formed. Interestingly, the βOH group of βHOMeVal is stably fixed by the hydrogen bond with either the O=C group of this residue or of the Leu-8 residue in the solution as well as in the solid state.

The molecular conformations of Ab-E were analyzed at nonaqueous solid and DMSO solution states and might be very different from those at the aqueous or receptor-bound state. Therefore, the precise description on the molecular conformation–activity relationship will have to await the further detailed characterization of this molecule under various different environments. However, the results presented in this paper should be of interest in the consideration of the activity profile of the Ab-E molecule. It is important to note that the crystal structure of the Ab-E molecule shows a slim and rigid conformation stabilized by three intramolecular hydrogen bonds, while the molecular conformation in the DMSO solution is rather rounded and flexible, except for the conformation around the βHOMeVal-9 residue. Judging from the present results, it may be said that the combination of "rigid conformation" around Leu–βHOMeVal–Hmp and "soft conformation" of the remaining bond sequence is necessary for Ab-E molecule to reveal its biological activity. Within this context, it seems worthwhile to note that cyclosporin A, a potent immunosuppressant drug characterized by high N-methylation of amide bonds, assumes a ring conformation[20] similar to the present Ab-E and shifts its structure toward a much rounded conformation upon binding to cyclophilin, a receptor protein of cyclosporin A.[21] Since the same situation might also be applicable in the case of Ab-E, information on conformational flexibility is useful for drug design with improved and/or altered antifungal activities.

Experimental Section

Materials. Isolation and purification of Ab-E from the fermentation broth of *Aureobasidium pullulans* R106 were conducted as described in a previous paper.[1] The HPLC separation on a preparative ODS-silica gel column of Capcell Pack C18 and the elution with acetonitrile–water (7:3, v/v) gave pure Ab-E. Since Ab-E is insoluble in water, its crystallization and NMR measurements were done in nonaqueous solution. The structural elucidation has already been reported in a previous paper.[2b]

X-ray Single-Crystal Analysis. After various efforts, single crystals of Ab-E were grown from a mixture of hexane–propan-2-ol–acetonitrile (90:10:5, v/v/v) as colorless plates by slow evaporation at room temperature. Thermogravimetry and differential thermal analysis showed that the crystals contain no solvents of crystallization. For the subsequent X-ray work, a single crystal of dimensions 0.2 × 0.3 × 0.5 mm was used.

A summary of the crystallographic data is given in Table 6. The unit-cell dimensions were determined by a least-squares fit of 2θ angles for 25 reflections with $33° \leq 2\theta \leq 58°$, measured by graphite-monochromated Cu Kα radiation (λ = 1.5418 Å) on an automated diffractometer. The crystal density was measured by the flotation method using a H_2O–KI saturated H_2O mixture. Intensity data were collected in an ω–2θ scan mode using the same diffractometer; the backgrounds were counted for 5 s at both extremes of each reflection peak. Four standard reflections were monitored for every 100 reflection intervals throughout the data collection, showing a random variation of ±2% with no significant trends. The observed intensities were corrected for the Lorentz and polarization effects, but not for the absorption effect.

Direct application of the phase determination procedures by SHELXS-86[22] and MULTAN87[23] programs failed to give an E-map that could be reasonably interpreted. The phase problem of Ab-E was finally overcome by applying the vector search

(20) (a) Loosli, H. R.; Kessler, H.; Oschkinat, H.; Weber, H. P.; Petcher, T. J.; Widmer, A. *Helv. Chim. Acta* **1985**, *68*, 682. (b) Kessler, H.; Kock, M.; Wein, T.; Gehrke, M. *Helv. Chim. Acta* **1990**, *73*, 1818.

(21) (a) Weber, C.; Wider, G.; von Freyberg, B.; Traber, R.; Braun, W.; Widmer, H.; Wüthrich, K. *Biochemistry* **1991**, *30*, 6563. (b) Fesik, S. W.; Gampe, R. T. Jr.; Eaton, H. L.; Gemmecker, G.; Olejniczak, E. T.; Neri, P.; Holzman, T. F.; Egan, D. A.; Edalji, R.; Simmer, R.; Helfrich, R.; Hochlowski, J.; Jackson, M. *Biochemistry* **1991**, *30*, 6574.

(22) Sheldrick, G.M. SHELXS-86: *Crystallographic Computing 3: Data Collection, Structure Determination, Proteins and Databases*; Sheldrick, G. M., Kruger, C., Goddard, R., Eds.; Clarendon Press: Oxford, 1985; pp 184–189.

Table 6. Summary of Crystal Parameters and Intensity Data Collection

molecular formula	$C_{60}H_{92}N_8O_{12}$
molecular weight	1117.43
crystal system	monoclinic
space group	$P2_1$
a, Å	16.458(3)
b, Å	10.638(3)
c, Å	18.133(6)
β, deg	103.51(2)
V, Å^3	3087(1)
Z, molecules/unit cell	2
D (measd), g cm^{-3}	1.198(3)
D (calcd), g cm^{-3}	1.202
F(000)	1208
μ(Cu Kα), cm^{-1}	6.45
λ (Cu Kα), Å	1.5418
T of data collection, °C	15
scan speed in 2θ, deg min^{-1}	3
scan range in ω, deg	1.40 ± 0.15 tan θ
data range measd, deg	$2° < 2\theta < 130°$
no. of unique data measd	5808
no. of reflections with $\lvert F_o\rvert > \sigma(F_o)$	5553
no. of variables refined	1090
R	0.067
Rw	0.089
S	1.280

procedure in the PATSEE program[24] using the three-dimensional (3D) model of Ab-E, which was constructed on the basis of the didemnin B conformation.[6] A possible 3D structure of Ab-E fragment, revealed on an E-map, led to a sensible stepwise extension of the entire Ab-E structure by successive Fourier syntheses.

The positional parameters of non-H atoms were refined by a full-matrix least-squares method with isotropic thermal parameters and then by a block-diagonal least-squares method with anisotropic thermal parameters. The geometrically ideal positions of H atoms were calculated and included in the final refinement with isotropic thermal parameters; their electron densities, except for the methyl protons of Hmp-1 and MeVal-2 and -7 side chains, were ascertained on a difference Fourier map. The function of $\Sigma\omega(\lvert F_o\rvert - \lvert F_c\rvert)^2$ was minimized, and $\omega = 1.0/[\sigma(F_o)^2 + 0.04042\lvert F_o\rvert + 0.00020\lvert F_o\rvert^2]$ was used for the final refinement using 5553 independent reflections. Final R [$=\Sigma(\lvert F_o\rvert - \lvert F_c\rvert)/\Sigma\lvert F_o\rvert$], R_w [$= (\Sigma\omega(\lvert F_o\rvert - \lvert F_c\rvert)^2/\Sigma\omega\lvert F_o\rvert^2)^{1/2}$] and S [$=(\Sigma\omega(\lvert F_o\rvert - \lvert F_c\rvert)^2/(M - N))^{1/2}$, where M = no. of reflections with $\lvert F_o\rvert > \sigma(F_o)$ and N = no. of variables used for the refinement] are given in Table 6. None of the positional parameters of non-H atoms shifted more than their ESDs, and the residual densities in the final difference Fourier map were in the range of -0.31 eÅ^{-3} to 0.35 eÅ^{-3}. The UNICS program system[25] was used for structural refinement and other crystallographic calculations. The atomic scattering factors and terms of anomalous dispersion corrections were taken from ref 26.

NMR Spectroscopy. All NMR measurements (500 MHz for protons), except the temperature-dependence experiment, were performed at 292 K. Ab-E was dissolved in 0.5 mL of DMSO-d_6 and adjusted to a concentration of 9 mM. Chemical shifts were measured relative to internal TMS at 0.0 ppm.

Two-dimensional (2D) NOESY, DQF-COSY, and HOHAHA spectra were acquired in the phase-sensitive mode. The time-domain matrix consisted of 256 × 2048 complex data points and was zero-filled to obtain a frequency domain matrix of 512 × 2048 real data points. Thus, the spectra had digital resolutions of 6.10 Hz/point for the ω1 direction and 3.05 Hz/point for the ω2 direction. $^3J_{HNC\alpha H}$ coupling constants were extracted from the DQF-COSY spectrum. Spectrum was zero-filled to achieve a digital resolution of 0.4 Hz/point.

In order to follow direct single- and multiple-relayed through-bond connectivities successively, the HOHAHA spectra were recorded with a mixing time of 80 ms, which is slightly longer than usual. NOESY spectra were measured with mixing times of 200, 400, 600, and 800 ms to evaluate the effects of spin diffusion and coherent magnetization transfer.

Computational Molecular Modeling. 3D structures which satisfy the NOE constraints of the intramolecular proton pairs were constructed by dynamical SA calculations[18] using the program Discover-Insight[27] operating on a computer graphics. This SA method consists of the following three steps. In the first step, an initial structure of Ab-E was built with a completely random array of atoms. Then a target function was determined by terms of the force constants for the covalent bond ($F_{covalent}$), interproton distance (F_{NOE}) and repulsive van der Waals contact (F_{repul}). By the steepest and successive conjugate descent methods, the conformational energy was minimized. The system was simulated for 50 ps at 1000 K by solving Newton's equation of the motion. The global minimum of the target function was searched by first substantially increasing the force constants until they regained their full values. In the second step, the temperature was cooled down by stepwise until 300 K. During this stage, the van der Waals repulsion terms were set to be predominant. The third step was again energy-minimized to refine the obtained structure.

As input data for the F_{NOE} constraints, the proton–proton pairs were classified into three distance groups by reference to the NOE intensities measured at the mixing time of 400 ms by virtue of the program NMR2:[28] strong (1.8–2.5 Å), medium (1.8–3.5 Å) and weak (1.8–5.0 Å). The $(\langle r^{-6}\rangle)^{-1/6}$ distance-averaging method was used for equivalent protons. For distance constraints that involved nonequivalent methylene, methyl, and aromatic ring protons which could not be stereospecifically assigned, the pseudoatom treatment was used. All calculations of other potential functions were performed following the protocol in the program Discover using the standard parameters.[18] As input data for constructing 3D structures by SA calculations, 15 sequential, and 15 intra- and 8 interresidual NOEs were used. No other restraints such as ϕ torsion angles or hydrogen bonds in which NH groups participate were included in the calculations; they were used as indicators for estimating the reliability of 3D structures constructed.

In order to quantitatively assess the convergence of the SA calculations, the following parameters were considered: the RMS violation, RMS deviation, and energies. The RMS violation is defined as the RMS difference between interproton distances of the calculated structures and experimental constraints. The RMS deviation was calculated for specific atoms such as backbone chains or Cα atoms.

Supplementary Material Available: Figures of the crystal packing and the temperature dependences of NH and βOH protons (3 pages). This material is contained in libraries on microfiche, immediately follows this article in the microfilm version of the journal, and can be ordered from the ACS; see any current masthead page for ordering information.

(23) Debaerdemaeker, T.; Germain, G.; Main, P.; Tate, C.; Woolfson, M. M. MULTAN87: *A System of Computer Programs for the Automatic Solution of Crystal Structures from X-Ray Diffraction Data*; Univs. of York, England and Louvain, Belgium, 1987.

(24) Egert, E.; Sheldrick, G. M. *Acta Crystallogr., Sect. A* **1985**, *41*, 262.

(25) *The Universal Crystallographic Computing System-Osaka*; The Computation Center, Osaka University: Osaka, Japan, 1979.

(26) *International Tables for X-ray Crystallography*; Kynoch: Birmingham, England, 1974; Vol. IV.

(27) Insight II User Guide, Version 2.1.0, Biosym Tech. San Diego, 1992.

(28) NMR2 User Guide, New Methods Research Inc., NY, 1989.